



Stability Enhancement of Doubly Fed Induction Generator Using a Linear Quadratic Regulator

Anant Oonsivilai*, Oscar A. Zongo, and Rachadaporn Oonsivilai

Abstract— This paper proposes a linear quadratic regulator to stabilize the rotor speed of the doubly-fed induction generator which oscillates as a result of noises in the input speed. The speed loop in the conventional vector control is reduced ignoring doubly-fed induction generator converter dynamics. Laplace transform of the closed-loop speed control is used to design an optimal controller based on the linear quadratic regulator to damp oscillations of the speed caused by measurement noise in the reference input. The state-space linearization of the system is presented. The strategy is aimed at reducing variations in rotor speed and electromagnetic torque during fault and achieve stable operation thereafter. In the paper linear quadratic regulator is compared with vector control and pole placement controller in terms of performances. The proposed controller improves the transient behavior of the induction machine when subjected to measurement noise. The recommended procedure maintains the stability of the wind generator during and after measurement noise. Results show the robustness of the linear quadratic regulator over other methods in tracking the reference values.

Keywords— DFIG, LQR, Oscillations damping, Speed and torque control.

1. INTRODUCTION

The doubly-fed induction generator (DFIG) [1]-[2] is widely used in wind energy conversion systems (WECS) as standalone [3]-[5] or in grid-connected mode [6]-[7]. In some cases, it is connected with some other renewable energy sources like solar photovoltaic to create a hybrid generation system supported by battery energy management system (BEMS) [8]-[10]. This is due to its ability to operate in variable speed, control active and reactive power, bidirectional power flow, low converter rating, high system efficiency, stator constant frequency, operate at sub-and super-synchronous modes and fault ride through (FRT) capability [8], [11]-[12].

In the past classical proportional integral (PI) controllers were used to control the DFIG in vector control and other methods. Nowadays modern controllers like optimal controllers are incorporated in the control of the DFIG. One of these optimal controllers is the linear quadratic regulator (LQR). There is an extensive application of LQR for DFIG control. The recent application is comparing the performance and costs of LQR and power system stabilizer in oscillations damping. In this work, Uncedented Kalman filter (UKF) is used to estimate unobservable states [13]. Particle swarm optimization is used to tune LQRI weighting matrices Q and R in [14]. The authors in [15] present a new method known as heightened state feedback control

(HSFC). This method is based on predictive control which is used to regulate rotor currents. The technique counteracts the dynamics caused by grid faults. Optimal preview based on LQR (LQR-OPC) is applied to damp power pulsations in a grid-connected DFIG [16]. To show its robustness the method is compared with sliding mode field-oriented control (SM-FOC) and direct torque control (SM-DTC). Results show that LQR-OPC has the best performance. Trajectory sensitivity analysis (TSA) is employed to find a suitable state weighting matrix for the LQR. The optimal controller obtained through this method significantly improves the settling of oscillation damping and makes the DFIG support grid voltage in the event of a fault [17]. Truncated Taylor series expansion is used to linearize a seven-order model of the DFIG to be used to obtain an optimal controller based on LQR. This controller controls the pitch, hence improve low voltage ride through capability of the DFIG and system damping even under severe disturbances [18]. Linear quadratic regulator's 18 weights of the diagonal matrix Q are tuned using PSO in [19], LQR is applied to damp sub-synchronous interaction in a farm of DFIGs [20].

The contributions of this paper are the improvement in the damping of the oscillations of DFIG using an optimal control approach and comparison between LQR Pole Placement in the stability enhancement. The linearization and the formulation of the state model of the system dynamics to form the state-feedback control law using LQR and Pole placement method is also explained in detail.

2. METHODOLOGY

First conventional vector control is explained in detail. Then a speed control loop for the DFIG is presented. From this loop, a transfer function representation of the system is obtained and used to find gains for optimal

Anant Oonsivilai is with the School of Electrical Engineering, Suranaree University of Technology, Nakhonratchasima, Thailand.

Oscar Zongo is with the School of Electrical Engineering, Suranaree University of Technology, Nakhonratchasima, Thailand.

Rachadaporn Oonsivilai is with the School of Food Technology, Suranaree University of Technology, Nakhonratchasima, Thailand.

*Corresponding author: Anant Oonsivilai; Phone: +66-91-415-3941; E-mail: anant@sut.ac.th, anant.oo141@gmail.com

controllers. Simulations are done for all three cases, that is, vector control, pole placement control and finally linear quadratic regulator control.

Direct and quadrature axes machine voltages and fluxes are given by, [21]:

$$v_{ds} = R_s i_{ds} - \omega_s \psi_{qs} + \frac{d\psi_{ds}}{dt} \quad (1)$$

$$v_{qs} = R_s i_{qs} + \omega_s \psi_{ds} + \frac{d\psi_{qs}}{dt} \quad (2)$$

$$v_{dr} = R_r i_{dr} - \omega_r \psi_{qr} + \frac{d\psi_{dr}}{dt} \quad (3)$$

$$v_{qr} = R_r i_{qr} + \omega_r \psi_{dr} + \frac{d\psi_{qr}}{dt} \quad (4)$$

Where v_{ds} and v_{qs} are the d -axis and q -axis of the stator and rotor voltages; R_s and R_r are the stator and rotor resistances; ω_s is the constant angular velocity of the synchronously rotating reference frame; ω_r is the rotor angular velocity;

$$\psi_{ds} = L_s i_{ds} + L_m i_{dr} \quad (5)$$

$$\psi_{qs} = L_s i_{qs} + L_m i_{qr} \quad (6)$$

$$\psi_{dr} = L_r i_{dr} + L_m i_{ds} \quad (7)$$

$$\psi_{qr} = L_r i_{qr} + L_m i_{qs} \quad (8)$$

where i_{ds} , i_{qs} , i_{dr} and i_{qr} are the d -axis and q -axis of the stator and rotor currents; ψ_{ds} , ψ_{qs} , ψ_{dr} and ψ_{qr} are the d -axis and q -axis of the stator and rotor fluxes.

Conditions for machine fluxes are:

$$\psi_{ds} = \psi_s \text{ \& } \psi_{qs} = 0 \quad (9)$$

Stator active and reactive powers are:

$$P_s = \frac{3}{2} (v_{ds} i_{ds} + v_{qs} i_{qs}) \quad (10)$$

$$Q_s = \frac{3}{2} (v_{qs} i_{ds} - v_{ds} i_{qs}) \quad (11)$$

In terms of rotor currents and synchronous speed, [22]

$$P_s = -\frac{3}{2} \frac{L_m}{L_s} v_{qs} i_{qr} \quad (12)$$

$$Q_s = \frac{3}{2} \frac{L_m}{L_s} v_{qs} (i_{ms} - i_{dr}) \quad (13)$$

where i_{ms} is the magnetizing current.

The electromagnetic torque is given by,

$$T_{em} = -\frac{3}{2} p \frac{L_m}{L_s} |\vec{\psi}_s| i_{qr} \quad (14)$$

The mechanical motion equation that describes the rotor speed behavior is,

$$\frac{d\omega_m}{dt} = \frac{p}{2J} (T_{em} - T_m) \quad (15)$$

where J is the inertia of the rotor and T_m is turbine aerodynamic torque.

Reference torque and rotor current can be generated from a given reference speed [23]. The error obtained is $\omega_m^{ref} - \omega_m$ processed by the proportional and integral controllers to give reference torque T_{em}^{ref} . This is multiplied with the gain G_1 to generate reference rotor current i_{qr}^{ref} . Then the transfer function TF_1 is used to obtain measured quadrature axis rotor current i_{qr} . This current is multiplied with the gain G_2 to obtain the required electromagnetic torque T_{em} . The error between electromagnetic torque T_{em} and the load torque T_m is multiplied by TF_2 to produce rotational mechanical speed Ω_m . Mechanical speed Ω_m is multiplied by the pole pairs p to obtain the required rotor speed ω_m .

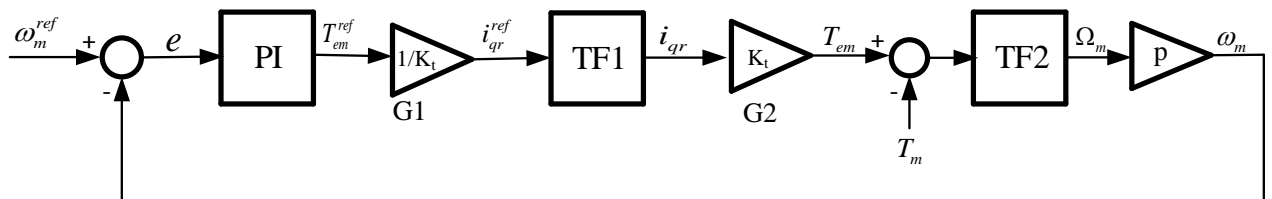


Fig. 1. The speed control loop of the RSC.

The torque constant is given by:

$$K_t = -\frac{3}{2} p \frac{L_m}{L_s} |\vec{\psi}_s| \quad (16)$$

The transfer function between the reference rotor current i_{qr}^{ref} and its measured value i_{qr} is [24]:

$$TF_1 = \frac{sk_p + k_i}{\sigma L_r s^2 + (k_p + R_r) s + k_i} \quad (17)$$

The transfer function between measured electromagnetic torque T_{em} and rotational mechanical speed Ω_m is given by,

$$TF_2 = \frac{1}{J s} \quad (18)$$

Closing the speed loop as shown in Figure 1 using the measured speed ω_m feedback and ignoring converter dynamics, it is obtained the closed loop transfer function $G(s)$ for speed using the proportional gain k_{pn} and integral gain k_{in} . The overall transfer function from ω_m^{ref} to ω_m is given by [23],

$$G(s) = \frac{sk_{pn} + k_{in}}{(J/p)s^2 + k_{pn}s + k_{in}} \quad (19)$$

The parameters of the PI controller are given by,

$$k_{pn} = \frac{2 \cdot \omega_n \cdot J}{p} \ \& \ k_{in} = \frac{\omega_n^2 \cdot J}{p}$$

where:

$$\omega_n = \frac{1}{\tau}$$

and τ is torque constant.

Pole placement method

This method is used to obtain the gains of the controller for the speed loop of the RSC of the DFIG shown in Figure 1. The state variables are fed back to the system through a regulator with constant gains [25]. This damps oscillations in the system.

In state variable form the system is,

$$\dot{x}(t) = Ax(t) + Bu(t) \quad (20)$$

$$y = Cx(t) \quad (21)$$

Equations (20) and (21) can be diagrammatically represented by Figure 2 where A is the state matrix B is the input matrix, C is the output matrix, K is the controller, r is the system input and y is the output.

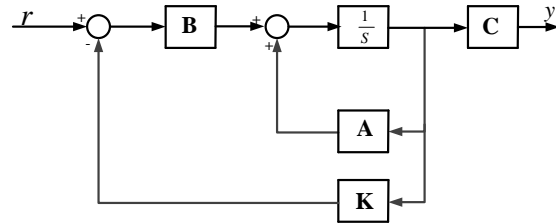


Fig. 2. System representation in state space.

The state feedback control,

$$u(t) = -Kx(t) \quad (22)$$

where K is $1 \times n$ vector of constant feedback gains.

With controller K , the system state-variable form becomes:

$$\dot{x}(t) = (A - BK)x(t) = A_f x(t) \quad (23)$$

The compensated system characteristic equation is,

$$|sI - A + BK| = 0 \quad (24)$$

The design objective is to find K in (24) which is the Pole Placement controller shown in Figure 3. Using Matlab function "placepol" the state feedback gain $K = [-2.3843 \ -2.6251]$ is obtained.

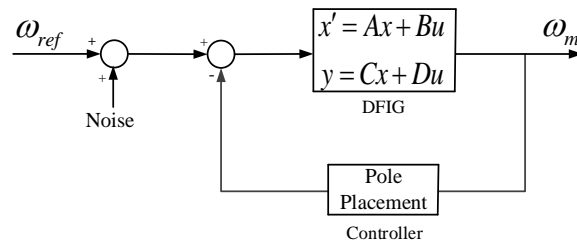


Fig. 3. The system with the pole placement controller.

Linear quadratic regulator

From the plant described by (20). The problem is to find the vector $K(t)$ of the control law:

$$u(t) = -K(t)x(t) \quad (25)$$

Which minimizes the value of a quadratic performance index J [13]-[15], [17]-[18], [25] of the form:

$$J = \int_{t=0}^{t=f} (x'Qx + u'Ru)dt \quad (26)$$

Subject to the dynamic plant (20).

Using n -vector Lagrange multipliers λ , the problem can be written as:

$$L(x, \lambda, u, t) = [x'Qx + u'Ru] + \lambda'[Ax + Bu - \dot{x}] \quad (27)$$

Equating the partial derivatives to zero,

$$\begin{aligned} \frac{\partial L}{\partial \lambda} &= AX^* + Bu^* - \dot{x}^* = 0 \\ \Rightarrow \dot{x}^* &= AX^* + Bu^* \end{aligned} \quad (28)$$

$$\begin{aligned} \frac{\partial L}{\partial u} &= 2Ru^* + \lambda'B = 0 \\ \Rightarrow u^* &= -\frac{1}{2}R^{-1}\lambda'B \end{aligned} \quad (29)$$

$$\begin{aligned} \frac{\partial L}{\partial x} &= 2x'^*Q + \dot{\lambda}' + \lambda'A = 0 \\ \Rightarrow \dot{\lambda}' &= -2Qx^* - A'\lambda \end{aligned} \quad (30)$$

Let:

$$\lambda = 2p(t)x^* \quad (31)$$

Substituting (22) into (29) gives the optimal closed-loop control law,

$$u^*(t) = -R^{-1}B'p(t)x^* \quad (32)$$

Obtaining the derivative of (30) gives,

$$\dot{\lambda}' = 2(\dot{p}x^* + p\dot{x}^*) \quad (33)$$

Finally, equating (30) with (33), we obtain:

$$\begin{aligned} \dot{p}(t) &= -p(t)A - A'p(t) - Q \\ &+ p(t)BR^{-1}B'p(t) \end{aligned} \quad (34)$$

Equation (34) is the matrix Riccati equation. Once the solution to (34) is obtained, the solution of the state equation (28) in conjunction with the optimum control equation (32) is obtained.

Implementation of LQR

Step 1: Parameters of the DFIG are substituted into the transfer function (19).

Step 2: The transfer function is converted to state space model using MATLAB to obtain the following matrices:

$$A = \begin{bmatrix} -160 & -100 \\ 64 & 0 \end{bmatrix}$$

$$B = \begin{bmatrix} 16 \\ 0 \end{bmatrix}$$

$$C = [10.0000 \quad 6.2500]$$

$$D = 0$$

Step 3: MATLAB function *lqr* is used to search for the controller gains $K = [-2.8423 \quad -0.9125]$.

The developed control system with noise in the input signal is as shown below:

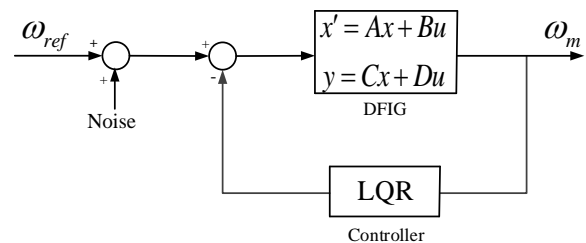


Fig. 4. The system with a linear quadratic regulator.

3. RESULTS, VERIFICATION AND DISCUSSION

The simulation experiment was conducted using the DFIG with the parameters shown in Table 1.

Table 1. Ratings and parameters of the DFIG

Parameter	Value
Real Power P	2 MW
Rotor Speed ω_m	1800 rpm
Number of Poles p	2
Stator Voltage V_s	690 V
Rotor Resistance R_r	0.0029 ohms
Stator Resistance R_s	0.26 ohms

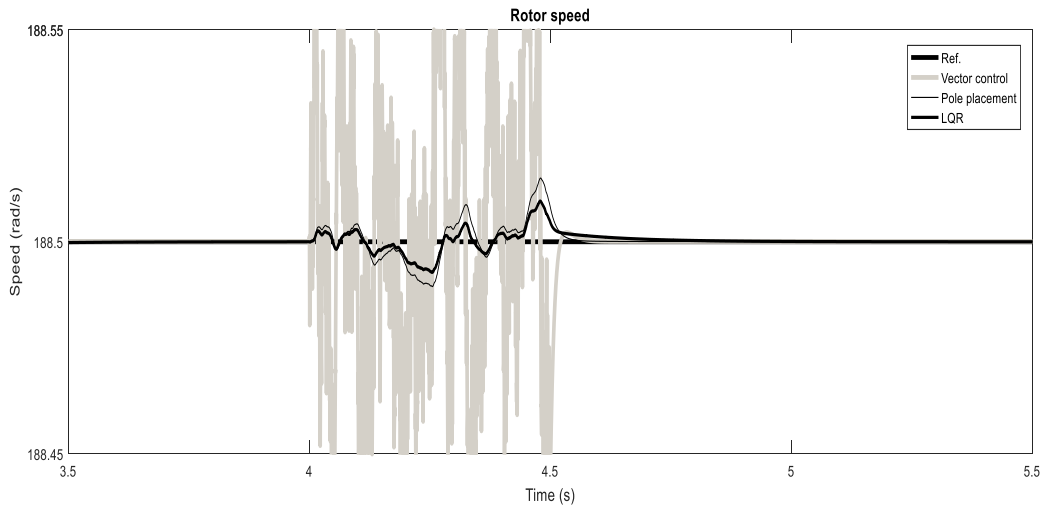


Fig. 5. Rotor speed of the DFIG with Vector control, with Pole placement controller and with LQR controller before fault, during fault and after the fault.

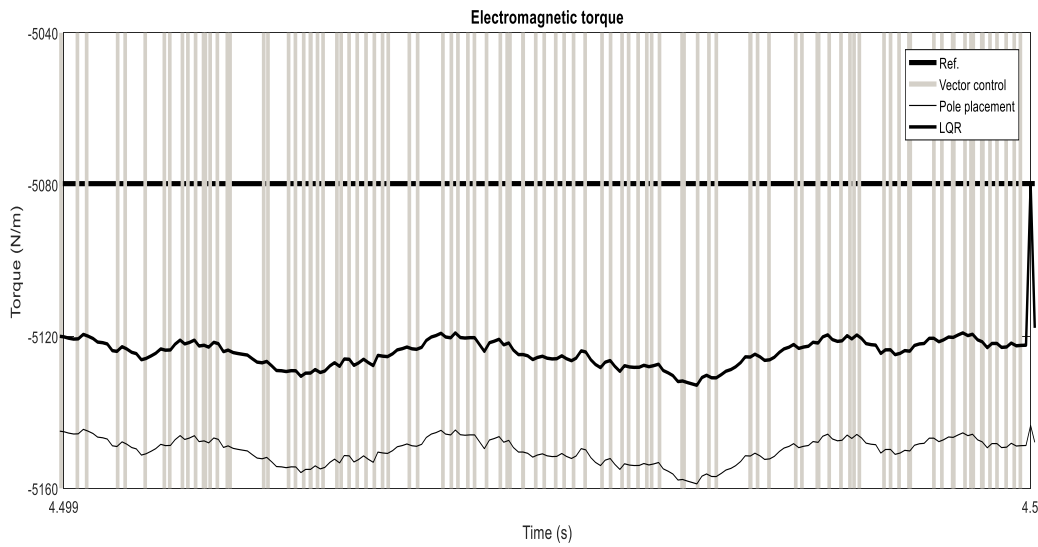


Fig. 6. Electromagnetic torque of the DFIG during the fault.

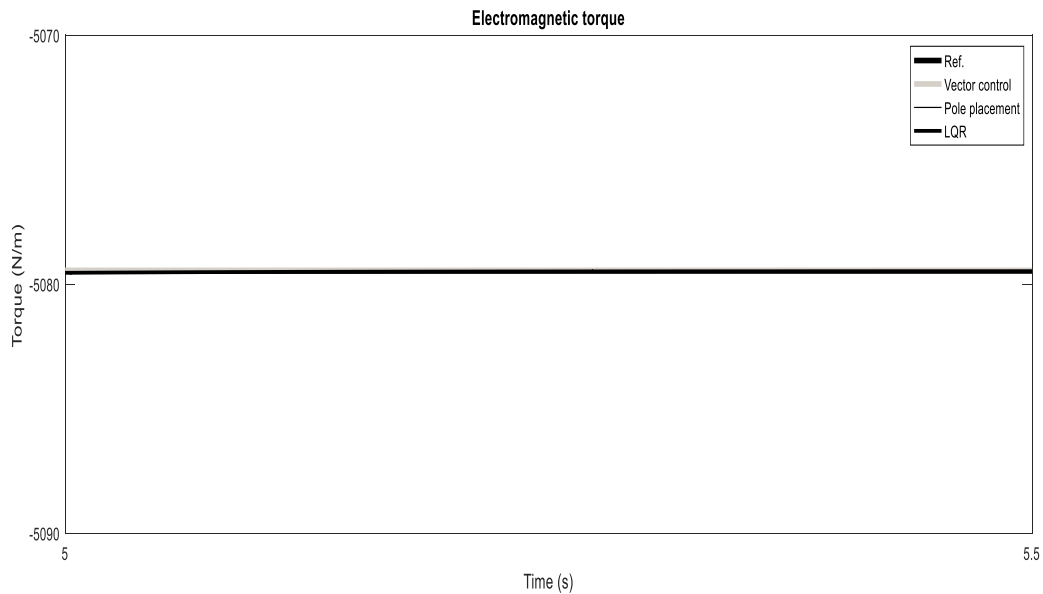


Fig. 7. Electromagnetic torque of the DFIG after the fault.

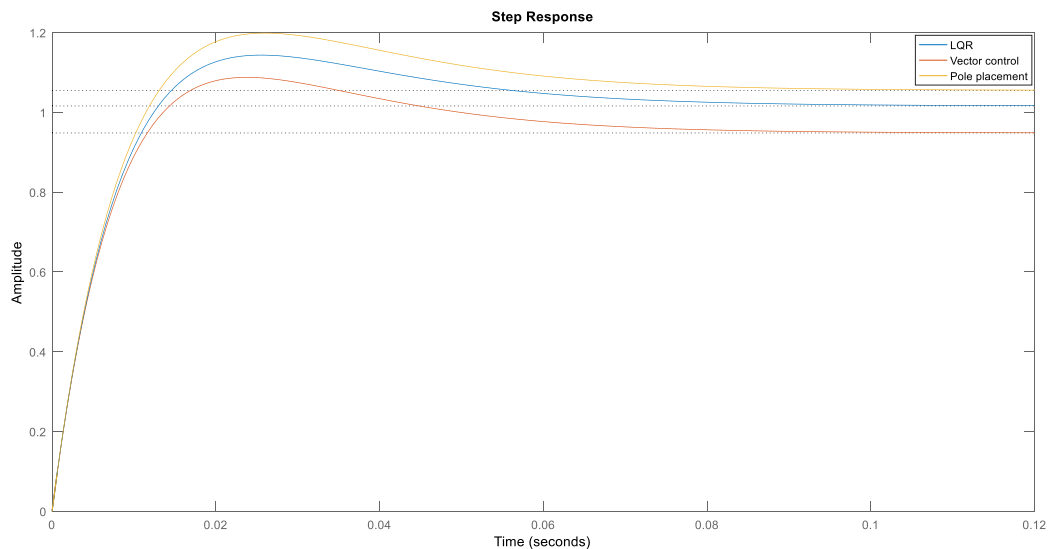


Fig. 8. Step response of the DFIG with Vector control, Pole placement and LQR.

Table 1. Step response results

Method	Overshoot	Settling Time	Rise Time	Steady State Error
LQR	12.5	0.0666	0.00853	0.948
Pole Placement	13.6	0.0674	0.00941	1.02
Vector Control	14.7	0.0686	0.0956	1.06

The efficacy of the proposed LQR controller to enhance stability has been found and compared with the vector control and pole placement. The control gains of the pole placement and LQR have been found by solving (24) and (34) with the help of the MATLAB.

Results

Simulations were done using the state space model of the system, with the pole placement controller and with the linear quadratic regulator. Noise in the input signal was added to check the stability of the system against disturbances.

With these controllers systems shown in Figure 3 and Figure 4 are run. Results are shown in Figure 5, Figure 6 and Figure 7.

Verification

The results are verified by step responses of the system as shown in Table 1 and Figure 8.

Discussion

Results in Figure 5, Figure 6 and Figure 7 show that LQR is robust compared to pole placement and vector control. During the fault, the speed of the DFIG with vector control has damaging oscillations when the input signal has noise from T=4s to T=4.5s. With the addition of optimal controllers, the speed plot has very small oscillations during fault, with LQR showing the best performance. The same situation is also experienced by electromagnetic torque during the fault. This shows that the stability of the studied system is improved with optimal controllers.

The step response of the system with the three methods shown in Figure 8 and Table 1 verify the results shown in Figures 5, 6 and 7. Step response show that LQR has the best performance with lowest overshoot, settling time, rise time and steady state error.

This study applies optimal controllers without the Kalman filter because all states are observable. In [13] UKF is applied to estimate unobservable states. But in both cases, the results show that LQR has the best performance in tracking the reference speed and stabilizing the torque during and after the fault. Although the studies have taken different approaches in both cases, this experiment and the experiment conducted by [17]-[18] the deviation of the speed for the conventional controller is very big during the fault. In [26] the electric torque and speed with and without LQR have similar behavior as results obtained in this study. That is there is a deviation during fault and stable before the fault. One of the significant achievements of this study is that all three controllers have fast response after fault, that rotor speed and torque track the reference values very fast after the occurrence of the measurement noises compared to the results obtained in [13], [15], [17]-[18].

4. CONCLUSION

In this paper, optimal controllers have been developed, which accounts for the noises in the reference speed of the doubly-fed induction generator wind turbine. Its development is based on applying optimal control design techniques of pole placement and linear quadratic regulator. The control strategy has been tested by a

disturbance from measurement noise. Simulation results have shown that the proposed scheme not only effectively controls the speed but also ensures stable electromagnetic torque after the occurrence of measurement noise in the reference input speed. Therefore, the proposed controller may be recommended as a candidate for wind turbine control.

ACKNOWLEDGMENT

This work is sponsored by Grants and Scholarships for Graduate Students through School of Electrical Engineering, Suranaree University of Technology, Nakhon Ratchasima, Thailand.

REFERENCES

- [1] Minh, Q. D.; Thanh, V. D.; Van T. N.; Hong V. P. N.; Ngoc T. N. T.; and Thi T. M. L. 2018. Effects of FSIG and DFIG Wind Power Plants on Ninh Thuan Power Grid, Vietnam. *GMSARN International Journal* 12: 133 – 138.
- [2] Phan, T. T.; Nguyen, V. L.; Huynh, P. T. and Tran, H. T. 2017. Dynamic Characteristics of the Doubly-Fed Induction Fed Induction Generator Based Wind Turbine under Grid Fault Conditions. *GMSARN International Journal* 11: 94 – 101.
- [3] Bhardwaj, P.; K. Vijayakumar. 2018. Modeling, operation and speed estimation of standalone wind driven doubly fed induction generator. In Proceedings of the Second International Conference on Inventive Systems and Control.
- [4] Xu, G.; Zhu, L.; and Pan Z. 2018. Virtual Synchronous Control using SOGI for standalone DFIG-based Wind Turbines with unbalanced and nonlinear loads. In 2018 21st International Conference on Electrical Machines and Systems (ICEMS) October 7-10, 2018, Jeju, Korea.
- [5] Misra, H. and Jain, A. K. 2018. Harmonics reduction in standalone DFIG-DC system by shunt active filter controlled in stator flux reference frame. In Indian Academy of Sciences.
- [6] Sahri, Y.; Tamalouzt, S.; Belaid S. L. 2018. Direct Torque Control of DFIG Driven by Wind Turbine System Connected to the Grid. 2018 In International Conference on Wind Energy and Applications. Algeria (ICWEAA).
- [7] Xiao, X.-Y.; Yang, R.-H.; Zheng, Z.-X.; and Wang, Y. 2019. Cooperative Rotor-Side SMES and Transient Control for Improving the LVRT Capability of Grid-Connected DFIG-Based Wind Farm. *IEEE Transactions on Applied Superconductivity*, Vol. 29, No. 2.
- [8] Li, Y.; Xu, Z.; Xiong, L.; Song, G.; Zhang, J.; Qi, D.; and Yang H. 2019. A cascading power-sharing control for microgrid embedded with wind and solar generation. *Renewable Energy* 132 (2019) 846e860.
- [9] Abdallah, I.; Gehin, A.-L.; and B. O. Bouamama. 2018. Event-driven Hybrid Bond Graph for Hybrid Renewable Energy Systems part I: Modelling and operating mode management. *International journal of hydrogen energy* 43: 22088 e22107.
- [10] Shaik, A. G.; and Mahela O. P. 201. Power quality assessment and event detection in a hybrid power system. *Electric Power Systems Research* 161: 26–44.
- [11] Bounar, N.; Labdai, S.; and Boulkroune A. 2018. PSO–GSA based fuzzy sliding mode controller for DFIG-based wind turbine. *ISA Transactions*.
- [12] M. E. Hossain. 2018. Low voltage ride-through capability improvement methods for DFIG based wind farm. *Journal of Electrical Systems and Information Technology* (5): 550–561.
- [13] Prajapat, G. P.; Senroy, N.; Kar, I. N. 2018. Stability enhancement of the DFIG-based wind turbine system through a linear quadratic regulator. *IET Generation, Transmission & Distribution*.
- [14] Murari, A.L.L.F.; Rodrigues, L.L.; Altuna, J.A.T.; Potts, A.S.; Almeida, L.A.L.; and Sguarezi F.A.J. 2019. LQRI power control for DFIG tuned by a weighted-PSO. *Control Engineering Practice* 85: 41–49.
- [15] Taveiros, F. E. V.; Barros, L. S.; F. B. Costa. 2019. Heightened state-feedback predictive control for DFIG-based wind turbines to enhance its LVRT performance. *Electrical Power and Energy Systems* 104: 943–956.
- [16] Subudhi, B.; and Ogeti, P. S. 2018. Optimal preview stator voltage-oriented control of DFIG WECS. *IET Generation, Transmission & Distribution*.
- [17] Abdelsalam, H. A.; Suriyamongkol, D.; and Makram, E. B. 2017. A TSA-Based Consideration to Design LQR Auxiliary Voltage Control of DFIG. In North American Power Symposium (NAPS).
- [18] Islam, K. S.; Shen, W.; Mahmud, A.; Chaudhury, M. A.; and Zhang J. 2016. Stability enhancement of DFIG wind turbine using LQR pitch control over rated wind speed. In *IEEE 11th Conference on Industrial Electronics and Applications (ICIEA)*.
- [19] Szypulski, M.; and Iwanski, G. 2016. Sensorless State Control of Stand-Alone Doubly Fed Induction Generator Supplying Nonlinear and Unbalanced Loads. *IEEE Transactions on Energy Conversion*, Vol. 31, No. 4.
- [20] Ghafouri, M.; Karaagac, U.; Karimi, H.; Jensen, S.; Mahseredjian, J.; and Faried S. O. 2017. An LQR Controller for Damping of Subsynchronous Interaction in DFIG-Based Wind Farms. *IEEE Transactions on Power Systems*, Vol. 32, no. 6.
- [21] Tang, C. Y.; Guo, Y.; and Jiang, J. N. Nonlinear Dual-Mode Control of Variable-Speed Wind Turbines with Doubly Fed Induction Generators. *IEEE Transactions on Control Systems Technology*, vol. 19, no. 4, July 2011.
- [22] Jang J-I, Kim Y-S , Lee D-C. Active and Reactive Power Control of DFIG for Wind Energy

- Conversion under Unbalanced Grid Voltage. 2006 CES/IEEE 5th International Power Electronics and Motion Control Conference.
- [23] Chen, Q-z; Defourny, M.; Bröls O. 2011. Control and simulation of doubly fed induction generator for variable speed wind turbine systems based on an integrated finite element approach. In Proceedings of the European Wind Energy Conference and Exhibition.
- [24] Vieira, J. P. A.; Nunes, M. N. A.; and Bezerra U. H. 2018. Design of Optimal PI Controllers for Doubly Fed Induction Generators in Wind Turbines Using Genetic Algorithm. In IEEE Power and Energy Society General Meeting - Conversion and Delivery of Electrical Energy in the 21st Century.
- [25] H. Saadat. 2011. Power system analysis. PSA Publishing LLC; 3rd edition.
- [26] Mohammadpour, H. A.; Ghaderi, A.; and Moham H. 2015. SSR damping in wind farms using observed-state feedback control of DFIG converters. *Electric Power Systems Research* 123: 57–66.
- [27] Thoa T. L.; and Dieu N. V. 2017. Optimal Layout for Off-shore Wind Farms Using Metaheuristic Search Algorithms. *GMSARN International Journal* 11: 1 – 15.
- [28] Trong T. P.; and Van L. N. 2016. RX Model-Based Newton Raphson Load Flow for Distribution Power System Considering Wind Farm with Asynchronous Generators. *GMSARN International Journal* 10: 11 – 18.